

# 琉球大学学術リポジトリ

## Radial Profile of the Surface Wind in the Typhoon-area

メタデータ	言語: 出版者: 琉球大学理工学部 公開日: 2012-02-28 キーワード (Ja): キーワード (En): 作成者: Ishijima, Suguru, 石島, 英 メールアドレス: 所属:
URL	<a href="http://hdl.handle.net/20.500.12000/23517">http://hdl.handle.net/20.500.12000/23517</a>

## Radial Profile of the Surface Wind in the Typhoon-area

Suguru ISHIJIMA\*

### Abstract

It is attempted in this paper to obtain the model of the radial wind profile within a typhoon whose position (latitude  $\varphi$ ) and whose pressure ( $P_0$ ,  $P_R$ ) and wind ( $V_0$ ,  $V_R$ ) at the inner radius  $r_0$  and at the external radius  $R$  are known. The model introduced here does not require the data of  $r_0$  because the boundary condition to be satisfied by the model yields the value of  $r_0$  as a function of other knowns ( $\varphi$ ,  $R$ ,  $V_R$ ,  $P_R$ ,  $V_0$ , and  $P_0$ ). The pressure profile is also automatically derived from the obtained wind profile. The validity of the model is checked by applying it for the cases of two typhoons. The computed wind and pressure radial distributions are generally supported by the available observational data, excepting the cases in which input data of  $V_0$  are not appropriately selected for computation.

### 1. Introduction

For the theoretical interest in obtaining the wind profile in the typhoon area one should seek for a solution of the equation of motion which satisfies the requirement of energy balance concerning the whole typhoon system, as done by Malkus and Riehl (1), Miller (2), etc.. However, unless such the special storm observation project as referred by these workers are at hand there always lies a difficulty to evaluate whether the obtained expression of the wind fits for the actual wind distribution due to the rarity of the observations in the typhoon atmosphere.

On the other hand, various empirical treatments have been performed to decide the wind formula that fit the results of the analysis of the available wind data, as seen in the works of Horiguchi (3), Takahashi (4), Hughes (5), Graham and Hudson (6), etc.. However, since these workers dealt with the particular stage of the typhoon life and with the particular region on the typhoon track, so obtained formula can only be meaningful for the particular cases or condition that they picked up for the analysis.

At present there exist two types of routine data available of the typhoon surface structure; one is data obtained by ships or at the land stations which were incidentally passed over by typhoons and the other is those supplied by the

---

Received : Oct. 31, 1974

\* Junier College Div. (Geophysical Science), Univ. of the Ryukyus

typhoon reconnaissance flights. When a typhoon stays over the ocean in the low latitude, the former type of data are normally expectable only in the typhoon peripheral region. The data of the central region are provided by the latter type. All the data we have for the formulation of the wind profile model are such elements as the peripheral pressure and wind, the size of the typhoon area, the center position, the central pressure and the maximum wind. The purpose of this paper is to obtain the simplified wind model but applicable for any stage of the typhoon without losing consistency with the horizontal equation of motion once when the data of such elements as above are provided.

## 2. Formulation of the model

The equation of horizontal motion is given by

$$\frac{\partial \mathbf{V}}{\partial t} + (\mathbf{V} \cdot \nabla) \mathbf{V} + \mathbf{f} \times \mathbf{V} = -\frac{1}{\rho} \nabla P + \mathbf{F} \quad (1)$$

, where  $f$  is Coriolis parameter,  $P$  atmospheric pressure,  $\rho$  air density,  $\mathbf{V}$  horizontal wind vector,  $\mathbf{F}$  vector of frictional force and  $\mathbf{k}$  unit vector in the vertical axis. Under the condition of steady and frictionless motion, Eq. (1) becomes

$$\nabla \left( \frac{1}{2} \mathbf{V}^2 + \frac{P}{\rho} \right) + \mathbf{k} \cdot \mathbf{V} = 0 \quad (2)$$

Assuming that the isobar pattern is circular to which the wind is everywhere tangential and rewriting the above equation in the polar coordinate we obtain

$$\frac{\partial}{\partial r} \left( \frac{1}{2} V^2 + \frac{P}{\rho} \right) - \mathbf{k} \cdot \mathbf{V} = 0 \quad (3)$$

, where  $\mathbf{k} = f + (\nabla \times \mathbf{V})_z = f + \frac{1}{r} \frac{\partial (Vr)}{\partial r}$ . Integration of Eq. (3) from the inner radius  $r=r_0$  to the external radius  $R$  yields;

$$\frac{P_R}{\rho} + \frac{1}{2} V_R^2 - \left( \frac{P_0}{\rho} + \frac{1}{2} V_0^2 \right) = \int_{r_0}^R \mathbf{k} \cdot \mathbf{V} dr \quad (4)$$

The solution of Eq. (4) was originally derived by James (7) for the case of  $V_R = 0$  using the energy ratio  $\frac{\rho}{2} V_0^2 / (P_R - P_0)$ . A similar type of expression can, however, be proved to be applicable for  $V_R \neq 0$ , and then we have for  $r_0 \leq r \leq R$

$$V = (r/r_0)^{-B} (V_0 + f B (1+B)^{-1} r_0) - f B (1+B)^{-1} r \quad (5)$$

assuming that the energy ratio  $B$  is given by  $B = \frac{1}{2} \rho (V_0^2 - V_R^2) / (P_R - P_0) = \frac{1}{2} \rho (V_0^2 - V_R^2) / (P_R - P_0) = \text{Const.}$ . We can also obtain the pressure profile

expressible in the form:

$$P = P_R - \frac{1}{2B} (V^2 - V_R^2) \quad (6)$$

The terms with suffixes 0 and R denote the values of the corresponding terms evaluated at  $r = r_0$  and  $r = R$ . The features of Eq. (5) are that the profile takes the maximum wind  $V_0$  at  $r = r_0$  and decreases from it to the wind  $V_R$  observed at external boundary  $r = R$  at the decreasing rate largely proportional to  $r^{-B}$  near the inner radius and at the enhanced decreasing rate near the external radius reflecting the effect of the second term in the right of Eq. (5).

At  $r=R$  Eq. (5) can be given as below in term of  $X = (r_0 / R)^B$ ,

$$X^\alpha + \alpha \sigma \delta X = 1 + \alpha \delta \quad (7)$$

, where  $\alpha = B / (1+B)$ ,  $\sigma = V_0 / V_R$  and  $\delta = V_R / f R$ . The above boundary condition is used to determine  $X$ , accordingly  $r_0$ , for given values  $B$ ,  $\sigma$  and  $\delta$ . An approximate solution for  $X$  in Eq. (7) can be obtained with aid of electronic computer by repetition of calculation with every decrement of  $X$  starting from the value 1 that is the largest value that it can take.

Table 1. The dependence of  $r_0$  upon  $B$  for the case in which  $\varphi = 20^\circ$  N,  
 $f = 4.965 \cdot 10^{-5} \text{ sec}^{-1}$ ,  $R = 374 \text{ km}$ ,  $fR = 14.3 \text{ m/s}$ ,  $\delta = 0.7$ ,  $V_R = 12 \text{ m/s}$ .

$\sigma$	$B$	$P_R - P_0 \text{ (mb)}$	$r_0 \text{ (km)}$
$(V_0 = 48 \text{ m/s})$	0.5	21.6	44.0
	0.4	27.1	23.7
	0.3	36.0	7.6
	0.2	54.0	0.7
$(V_0 = 60 \text{ m/s})$	0.5	34.6	31.5
	0.4	43.2	15.9
	0.3	57.6	4.3
	0.2	86.4	0.4

An example of the dependence of  $r_0$  upon  $B$ , accordingly upon  $V_0$  and  $P_R - P_0$  is shown in Table 1 for the case in which the storm center is situated at a fixed point with the size and peripheral wind being kept constant (for instance,  $\varphi = 20^\circ$  N,  $R = 374 \text{ km}$  and  $\delta = 0.7$ ), changing  $B$  for the breakdown of  $\sigma$ . It is observed that the value of  $r_0$  decreases as  $B$  decreases, that is, as the depth of

pressure  $P_R - P_0$  increases. It is also revealed in Table 1 that the increase in  $\sigma$ , that is, the increase in  $V_0$  keeping  $B$  constant tends to show the decrease in  $r_0$ . The concept implied in the above results are well supported by the conclusion given by Shimada (8) as a result of his analysis of Typhoon (Louise) 5522 that the size of eye radius, an indicator of the position of maximum wind, shrinks and spreads as the central pressure falls and rises, respectively.

### 3. Computed radial wind-profile in the typhoon area

Such data as  $f$ ,  $R$ ,  $V_R$ ,  $P_R$ ,  $V_0$  and  $P_0$  need to be prepared as the input for computing the radial wind profile from Eq. (5) and Eq. (7). The data of  $R$ ,  $P_R$ , and  $V_R$  are obtained from the analysis of Japan Far East Surface Weather Map and those for other terms are from the summary report of typhoon flight reconnaissance.  $R$  is defined as the mean of the largest closed isobar  $R_1$  and that of its next smaller isobar  $R_2$  in the Map drawn in 4 mb interval contour.  $V_R$  is estimated as the gradient wind computed from the radial gradient 4 mb / ( $R_1 - R_2$ ).  $P_R$  is given by the pressure on the closed iso-bar with the radius  $R$ .  $V_0$  is the frictionless maximum wind that can be approximated

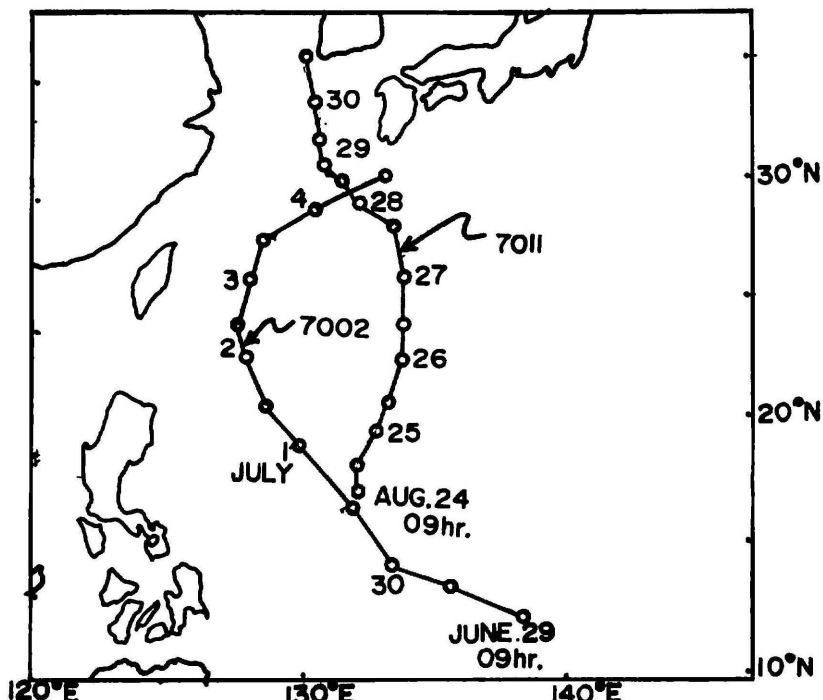


Fig. 1. The tracks of the typhoons picked up for analysis.

7002 and 7011 denote No. 2 and No. 11 typhoons occurred in 1970.

with the maximum gust wind which can be estimated to be the mean maximum wind provided by the typhoon reconnaissance but multiplied by 1.38 which is assumed to be the ratio of the maximum gust wind to the mean maximum wind. The ratio 1.38 is gained by James (7) from the analysis of several typhoons.  $P_0$  is alternated with the central pressure read from the curve connecting the central pressure reports of the flight reconnaissance.

The wind profiles for two typhoons (Typhoon 7002 and Typhoon 7011) are computed at 9 hr and 21 hr each day for the period when they stay over the ocean. Their tracks are indicated in Fig. 1. In Table 2 we prepared a list

Table 2. List of the input data for computation of the radial wind distribution and the computed values of  $B$  and  $r_0$  for Typhoon 7002

Date Jun.' 70	Lat. (deg)	R (km)	$V_p$ (m/s)	$P_0$ (mb)	$V_R$ (m/s)	$P_R$ (mb)	B	$r_0$ (km)
29 09	12.2	289	26.0(18.7)	995	19.3(13.9)	1006	0.168	68.1
29 21	13.0	300	42.2(30.4)	975	18.6(13.4)	1006	0.278	23.0
30 09	14.0	400	59.1(42.3)	960	19.1(13.8)	1006	0.408	39.9
30 21	16.0	311	39.4(28.4)	979	16.3(11.7)	1006	0.286	24.2
1 09*	17.9	500	89.4(64.4)	910	14.2(10.2)	1006	0.487	26.9
1 21*	19.4	533	90.1(64.9)	905	15.5(11.2)	1006	0.468	30.7
2 09*	21.0	566	84.5(60.8)	910	14.4(10.4)	1006	0.433	28.9
2 21*	22.4	366	71.8(51.7)	935	18.0(13.0)	1002	0.433	29.4
3 09*	24.3	355	54.9(39.5)	955	19.9(14.3)	1002	0.334	33.6
3 21*	26.0	366	45.0(32.4)	955	14.5(10.4)	1002	0.232	8.7
4 09*	27.7	311	42.2(30.4)	950	11.8( 8.5)	1002	0.190	1.5

\* July

of the input data necessary for computation in the left and the computed values of  $B$  and  $r_0$  are in the right for the case of Typhoon 7002. The flight data of the mean maximum wind are so fluctuating and so intermittently observed as shown in Fig. 2 that smoothing was inevitable to gain the values at every 9 hr and 21 hr, disregarding the abnormally deviated ones. The values of  $V_0$  in Table 2 are 1.38 times of those read from the smoothed maximum wind curve shown by solid line in Fig. 2. The mean maximum wind are shown in the parentheses. The smoothing was not made for the case of the depth of the pressure though its data being considerably fluctuating, because the pressure data is much more reliable than the mean maximum wind. The computed  $B$  showed

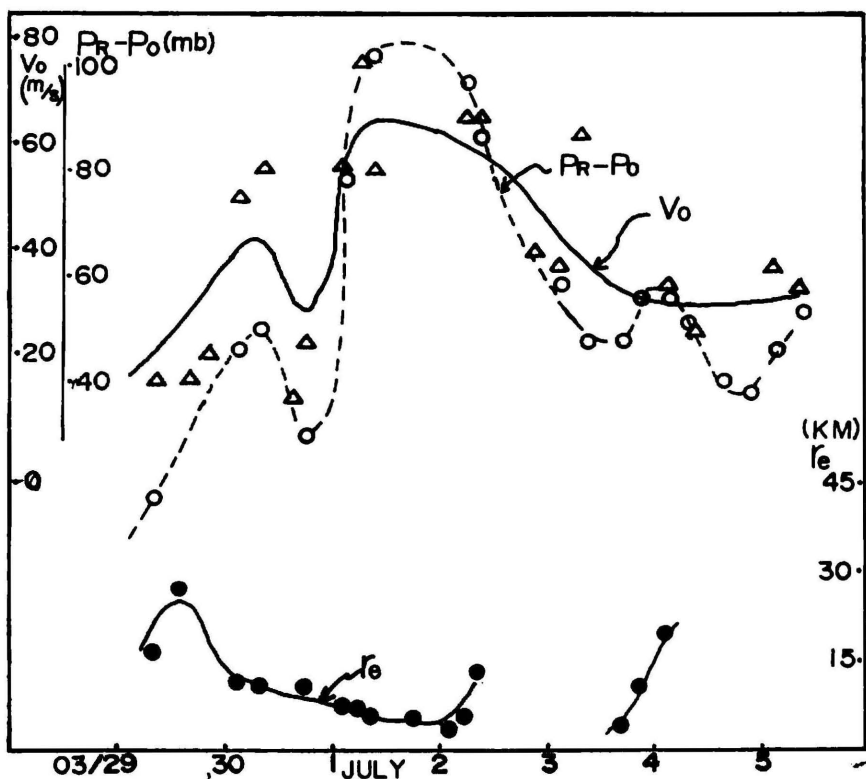


Fig. 2. Variations of the mean maximum wind  $V_0$ , depth of the pressure  $P_R - P_0$  and the size (radius) of eye  $r_e$  for the case of Typhoon 2002.

the variation from 0.17 to 0.49 with the smaller values in the both early and decaying stages and the larger in the mature stage. According to Hughes's work (5) the values of  $x$  in the profile expression  $r^{-x}$  would be somewhat smaller than 0.62 in the inner region  $r < 1^\circ$  lat. distance. We find that this agrees with the result of the present study for the case of mature stage, considering that the present model becomes  $r^{-B}$  when  $r$  is small. In Fig. 3 are presented the variation of the computed radial wind profiles for the whole period of the analysis. In the figure the wind speed with 28 percent discount of the original computed wind speed are given, taking into the effect of the frictional force which was neglected in the equation of motion expressed by Eq. (2), together with all available data of the surface wind in or near the typhoon domain. In addition, for the reference sake, the computed pressure profiles from Eq. (6) are demonstrated together with the pressure distribution obtained from the isobar contour pattern of the Map whose trend is shown in Fig. 3 by a pair of solid circles.

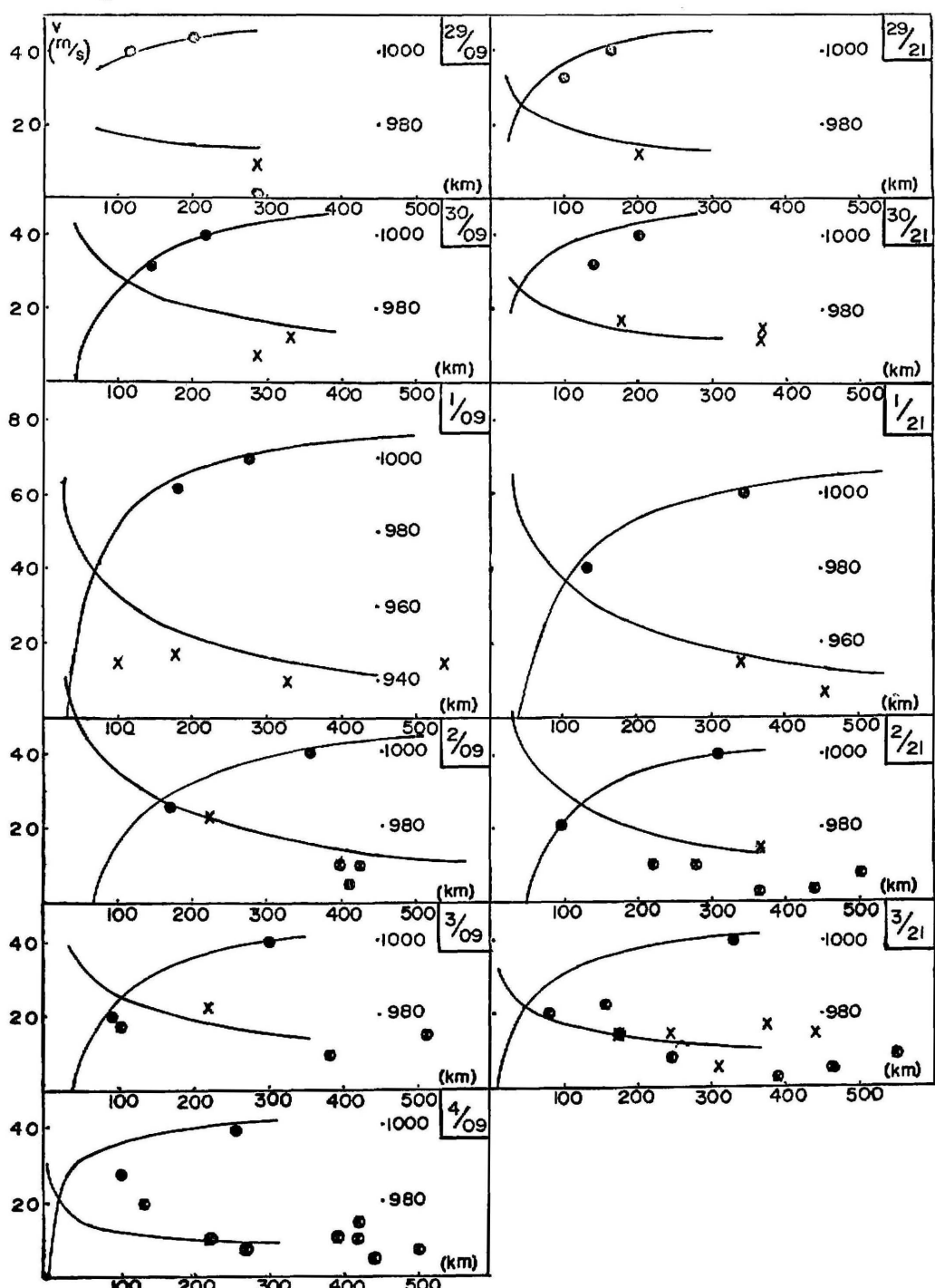


Fig. 3. Computed wind and pressure distributions for the case of Typhoon 2002 every 9 hr(right) and 21 hr (left) during the analysis period.

Table 3. List of the input-data for computation of the radial wind distribution and the computed values of  $B$  and  $r_0$  for Typhoon 7011

Date Aug. '70	Lat. (deg)	R (km)	$V_0$ (m/s)	$P_0$ (mb)	$V_R$ (m/s)	$P_R$ (mb)	B	$r_0$ (km)
24 09	16.5	577	23.2(16.7)	990	13.3( 9.6)	1006	0.136	39.5
24 21	17.4	555	37.3(26.9)	975	14.4(10.4)	1006	0.229	26.9
25 09	18.8	599	47.9(34.5)	965	15.8( 1.4)	1006	0.299	45.5
25 21	20.4	622	54.2(39.0)	960	13.4( 9.6)	1006	0.360	48.6
26 09	22.1	455	58.4(42.0)	935	17.1(12.3)	1002	0.398	47.8
26 21	23.7	488	53.5(38.5)	960	18.0( 3.0)	1002	0.362	54.3
27 09	25.4	544	61.2(44.1)	950	15.7(11.3)	1002	0.404	60.3
27 21	27.0	588	62.6(45.1)	945	14.4(10.4)	1002	0.391	56.5
28 09	27.9	544	57.7(41.5)	945	16.2(11.7)	1002	0.323	39.9
28 21	28.9	544	52.1(37.5)	950	15.3(11.0)	1002	0.286	33.4
29 09	29.7	500	47.9(34.5)	950	16.0(11.5)	1002	0.235	21.1
29 21	3.0	466	44.3(31.9)	965	13.7( 9.9)	1002	0.227	13.8

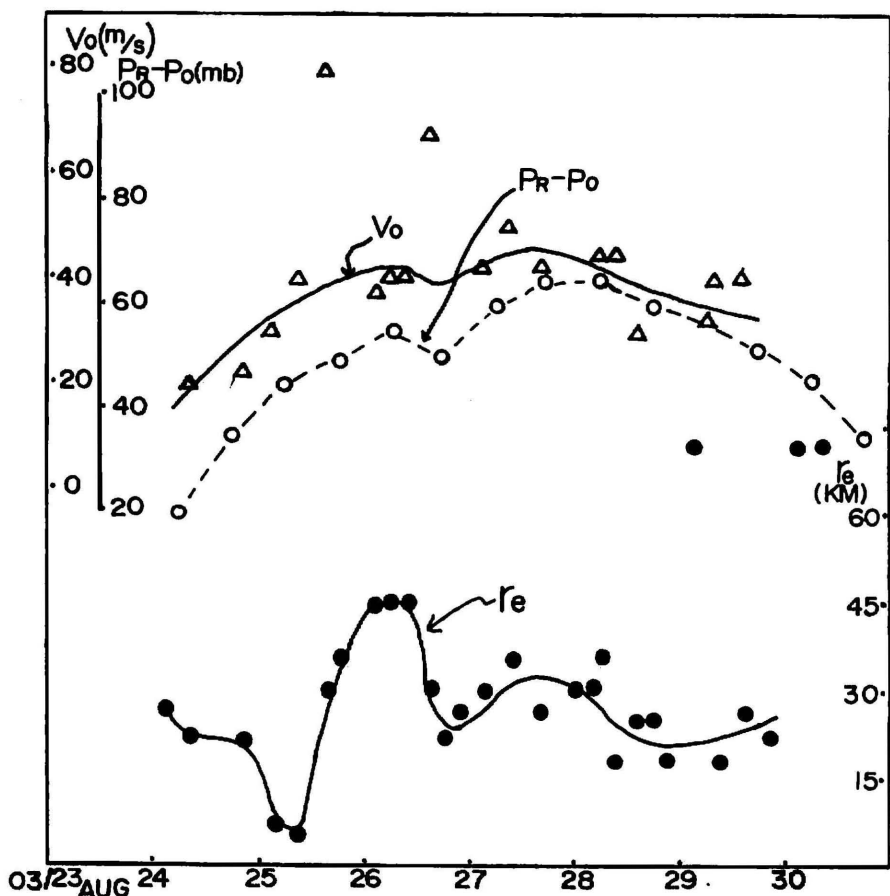


Fig. 4. Variations of the mean maximum wind, the depth of the pressure and the size (radius) of eye for the case of Typhoon 7011.

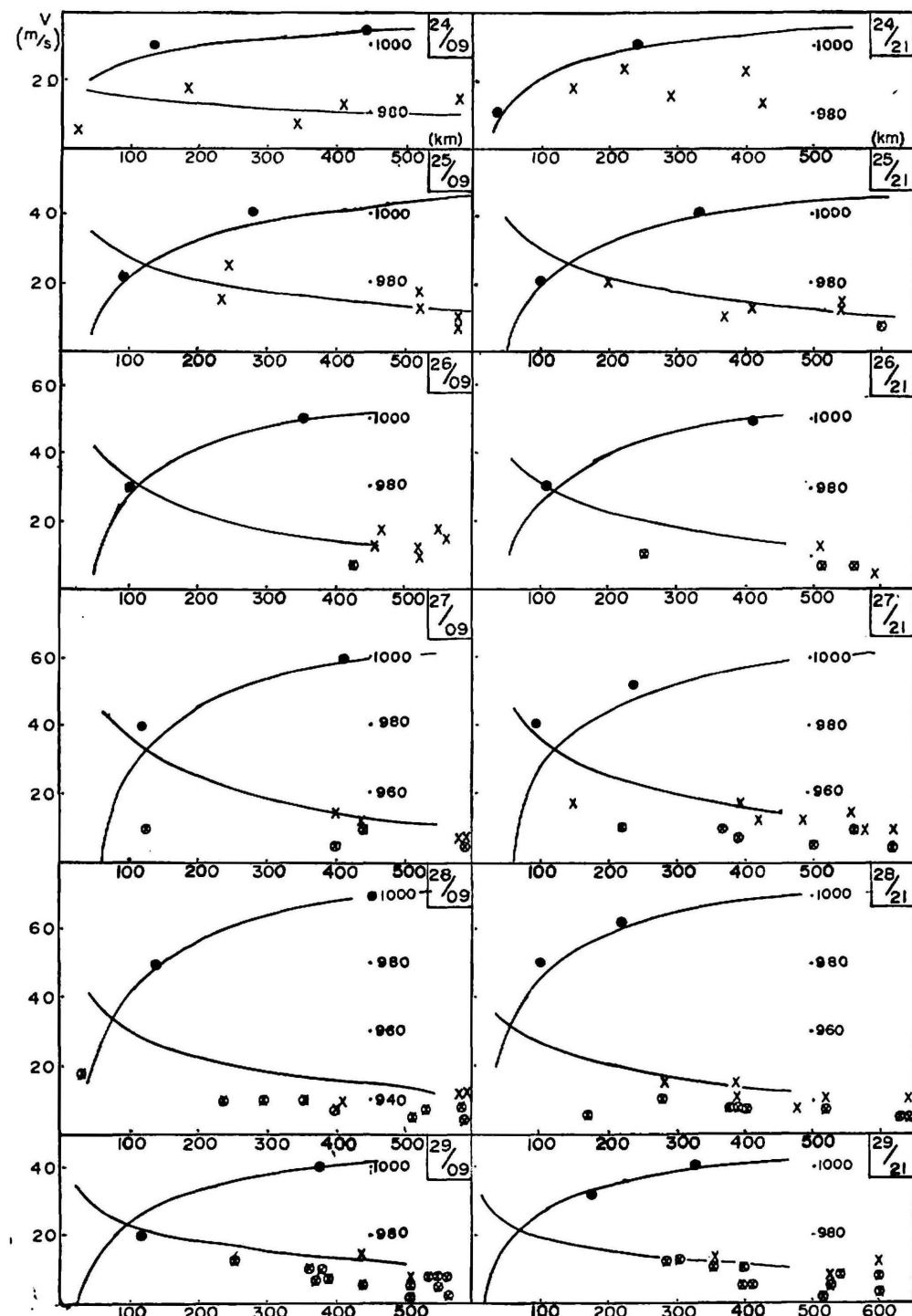


Fig. 5. Computed wind and pressure distributions for the case of Typhoon 7011 at 9 hr (right) and 21 hr (left) each day during the analysis period.

The same was processed for the case of Typhoon 7011. The input data and the computed values of  $B$  and  $r_0$  are shown in Table 3 and the computed wind and pressure profiles are in Fig. 5. The variations of the mean maximum wind and the depth of the pressure are shown in Fig. 4. It is observed that the mean maximum wind data are much more steady than those of Typhoon 7002 which made it easy to figure out the trend of maximum wind.

#### 4. Discussion

The computed values of  $r_0$  are compared in Fig. 6 with the observed eye radius  $r_e$ , for the maximum wind is generally known to occur near outside the eye radius. In the figure the values obtained from the analysis of other

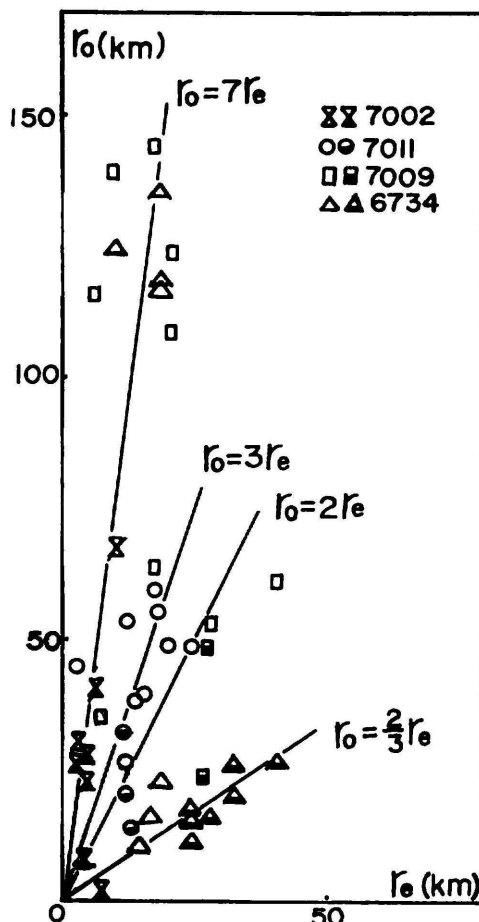


Fig. 6. The relation between the computed distance of the maximum wind occurrence  $r_0$  and the observed eye radius  $r_e$ . The blank mark sare for the earlier stage and the half solid marks for the later stage of the analysed typhoons.

typhoons (Typhoon 7009 and Typhoon 6734) are added in. It is observed that all four cases the computed values are larger than the observed eye radius. The computed values of  $r_0$  are several times of the observed eye radius in the developing stage but the two come closer in the decaying stage. However, in the latter stage adoption of underestimated values of  $V_0$  might have caused the smaller values of  $r_0$  as seen in Table 1. If for instance we take 48 m/s and 36 mb in place of the correct values of 60 m/s and 36 mb for  $V_0$  and  $P_R - P_0$ , respectively, the value of  $r_0$  would come out 7.6 km, while the adoption of the correct values give us about 30 km for  $r_0$ . By the way in the decaying stage we have probably made a lower estimation of  $V_0$  due to our subjective mind which tends to reduce down the value in extrapolation giving much weight on the decaying tendency. If we admit this point and select the larger values of  $V_0$  the values of  $r_0$  in that period would have come out larger. Accordingly, it can be expected that occurrence of the maximum wind would appear in the distance several times of the eye radius away from the storm center. A further discussion, however, can not be made on this matter until more reliable data and knowledge on the variations of  $V_0$  and the size of eye radius are obtained.

It is difficult to verify whether the computed profiles of wind are supported by the observational data, because the amount of the surface wind data is so much limited in the typhoon domain and there is the difference in the source of the data. The data reported by the land stations are shown by circled crossings and those by ships are presented by crossings in Fig. 3 and Fig. 5, without making any correction, for instance, to convert the observed values at the land stations into the status of the ship observation. Under such circumstances, when we examine in Fig. 3 and Fig. 5 the computed radial profiles in relation to the observational data, we must keep in mind that the observed values at the land stations are considerably smaller than those observed by ships and there are also some land stations which are deeply affected by the orographic effect, and that the aparted wind (weak and strong) data sometimes exist at the same distance from the center due to the asymmetrical nature of the typhoon. It should also be kept in mind that all the wind data are expressed in the error range 1.5 m/s, for the data were converted from the number of the barbs of the wind mark used in the synoptic weather map.

These limited amount of and, to be worse, worse quality of data, however, could help us to reach some conclusions. As for the case of Typhoon 7002, the computed wind profiles result in an overestimation of the wind in the developing stage (June 29 and 30) and agreement with the observational data

for the mature stage (from July 1 through July 2) and an underestimation in the decaying stage (from July 3 through July 4) especially in the inner region. Above points are naturally reflected upon the pressure profile yielding discrepancies between the computed profiles and the ones given in the Map. It is suggested that an overestimation appeared in the developing stage can be attributed to the adoption of the overestimated values of the maximum wind  $V_0$  during that period while the disagreeable profiles obtained for the decaying stage must be associated with an underestimation of  $V_0$  (Ref. Fig. 2). For the case of 21 hr June 30 of Typhoon 7002 the computed pressure profiles are extremely deviated from the map analysed data. This is due to the fact that the present computation was performed by taking into consideration the sudden weakenning appeared around that time observed as the filling of the central pressure which results in the decreasing in the depth of the pressure and as the decreasing of the maximum wind (Ref. Fig. 2).

As for the case of Typhoon 7011 we generally confirmed that the computed profiles of the wind and the pressure are far better expressive for the observational data than those for the case of Typhoon 7002, although the disagreeable pressure profiles are still revealed in the decaying stage as same as for the case of Typhoon 7002. This disagreement in the decaying stage might be resulted from adopting the underestimated values of  $V_0$  in extrapolating for the blank of the data. The major reason of the improvement found in the wind profile for the case of Typhoon 7011 over that of Typhoon 7002 lies in that the values of  $V_0$  used as the initial input data could more reliably be estimated for the former due to the steadiness found in the variation of its intensity.

##### 5. Concluding remarks

The surface wind structure in a typhoon area is not so simple as treated in this paper, but to formulate this we dared to stay with the simplified treatment that was possible under the minimum supply of the observational data. However, this naturally leads to the model that is unable to express the features that belong to the disregarded factors upon simplification. At this point we realized the difficulty to face with in examining whether the deviation of the computed profiles from what the available data would suggest are resulted from the exclusion of the complexity of the typhoon, or from the essential defect of the model itself. In order to clarify the former doubt, one should formulate the model that facilitates inclusion of the asymmetry of the typhoon and the speed of typhoon motion, simultaneous derivation of the radial wind component, more consistent treatment of frictional force, etc.. This work would, however, again

encounter the barrier of the rarity of the observational data, so long as one seeks for the model applicable for the whole span of a typhoon life.

The major benefit of the approach taken in this paper for obtaining the radial profile of the typhoon wind is found in that it starts with the isobar pattern in the typhoon peripheral region plus the minimum information on the center region which are usually in hand and that it works consistently for the whole period of the typhoon life.

### Acknowledgement

The author wishes to thank Prof. Kondo, Univ. of Tohoku, Prof. Sekioka, National Defence Academy and Dr. Nitta, Japan Meteorological Agency for their giving valuable suggestions to this work. The author also wishes to appreciate the staff of Electronic Computer Center, Univ. of the Ryukyus for their computation service indispensable for this work. Thanks are also due to Mr. Shinko Yamashiro who helped to draft the involved figures.

### References

- (1) Malkus, J. S. and H. Riehl, 1960: On the dynamics and energy transformations in steady state hurricanes. *Tellus* 12, 1-20.
- (2) Miller, B. I., 1962: On the momentum and energy balance of hurricane Helene (1959). National Hurricane Research Project, Report No. 53.
- (3) Horiguchi, Y., 1927: On the typhoon of the Far East. Part II. The Memoirs of the Imp. Mar. Obs. Kobe, 3.
- (4) Takahashi, K., 1939 Distribution of pressure and wind within typhoon area. *J. Meteor. Soc. Japan*, 17.
- (5) Hughes, A., 1952: On the low level wind structure of tropical storms. *J. Meteor.* 9, 422-428.
- (6) Graham, H. and G. Hudson, 1960: Surface winds near the centers of hurricanes (and other cyclones). National Hurricane Research Project, Report No. 39.
- (7) James, W., 1951: On the evolution of tropical cyclones. *J. Meteor.* 8, 17-23.
- (8) Shimada, K., 1962: Some problems in the use of data obtained by aircraft typhoon reconnaissance flights. Proceedings of the interregional seminar on tropical cyclone in Tokyo 18-31 Jan. 1962.